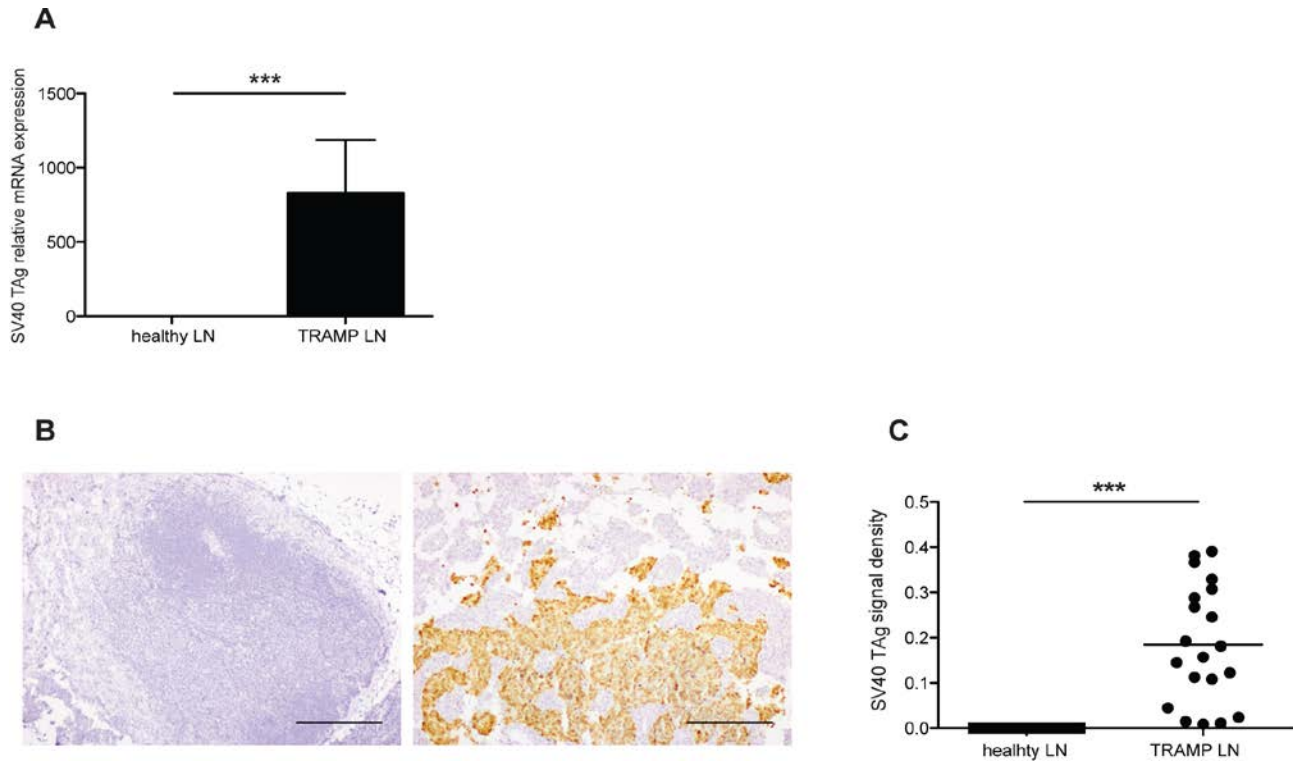


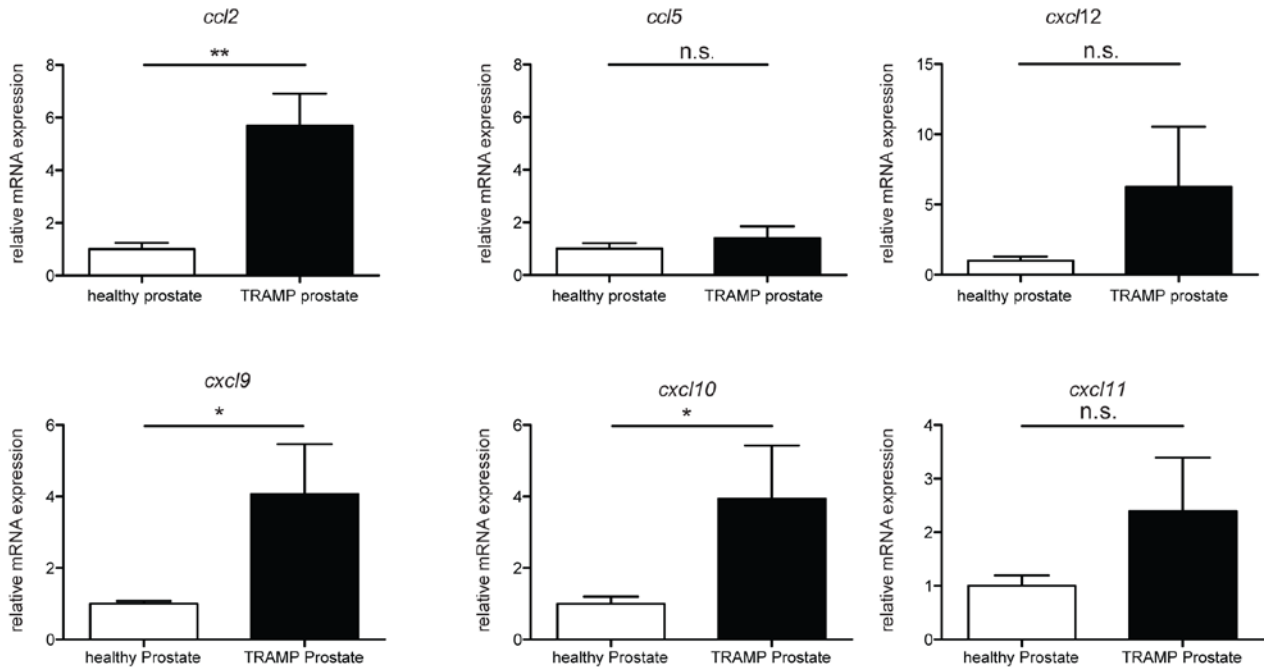
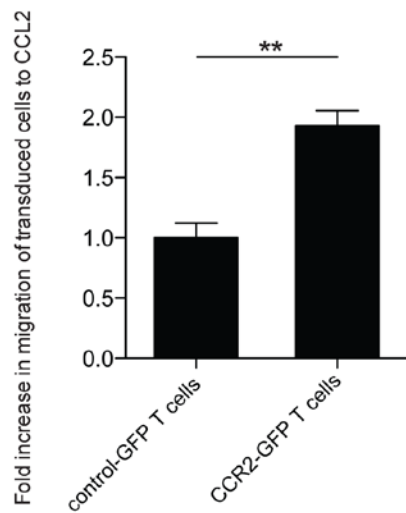
# Tailored chemokine receptor modification improves homing of adoptive therapy T cells in a spontaneous tumor model

## Supplementary Material



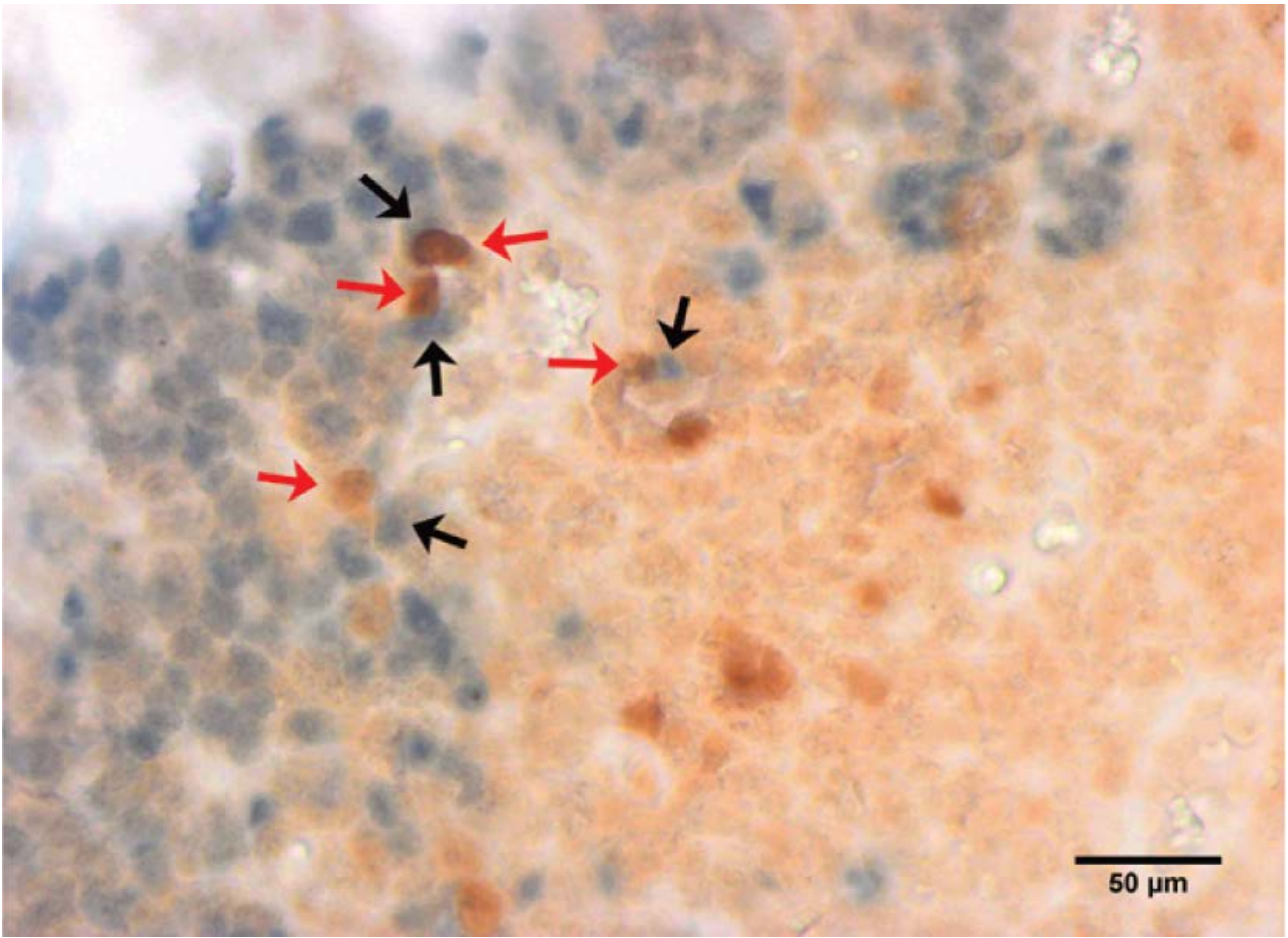
## Supplemental Figure 1

**A:** Representative mRNA expression of SV40 TAg genetic marker of TRAMP tumors, via real-time qPCR. Fisher's test (zero signal versus positive signal): (\*\*\*)  $P < 0.001$ . **B:** Representative images of immunohistochemical analysis of SV40 TAg on mouse lymph nodes from C57BL/6 (ctrl) or TRAMP mice bearing lymph node metastasis: Brown staining SV-40<sup>+</sup> cells. Original Magnification 20x. Scale bars: 100  $\mu\text{m}$ .

**A****B**

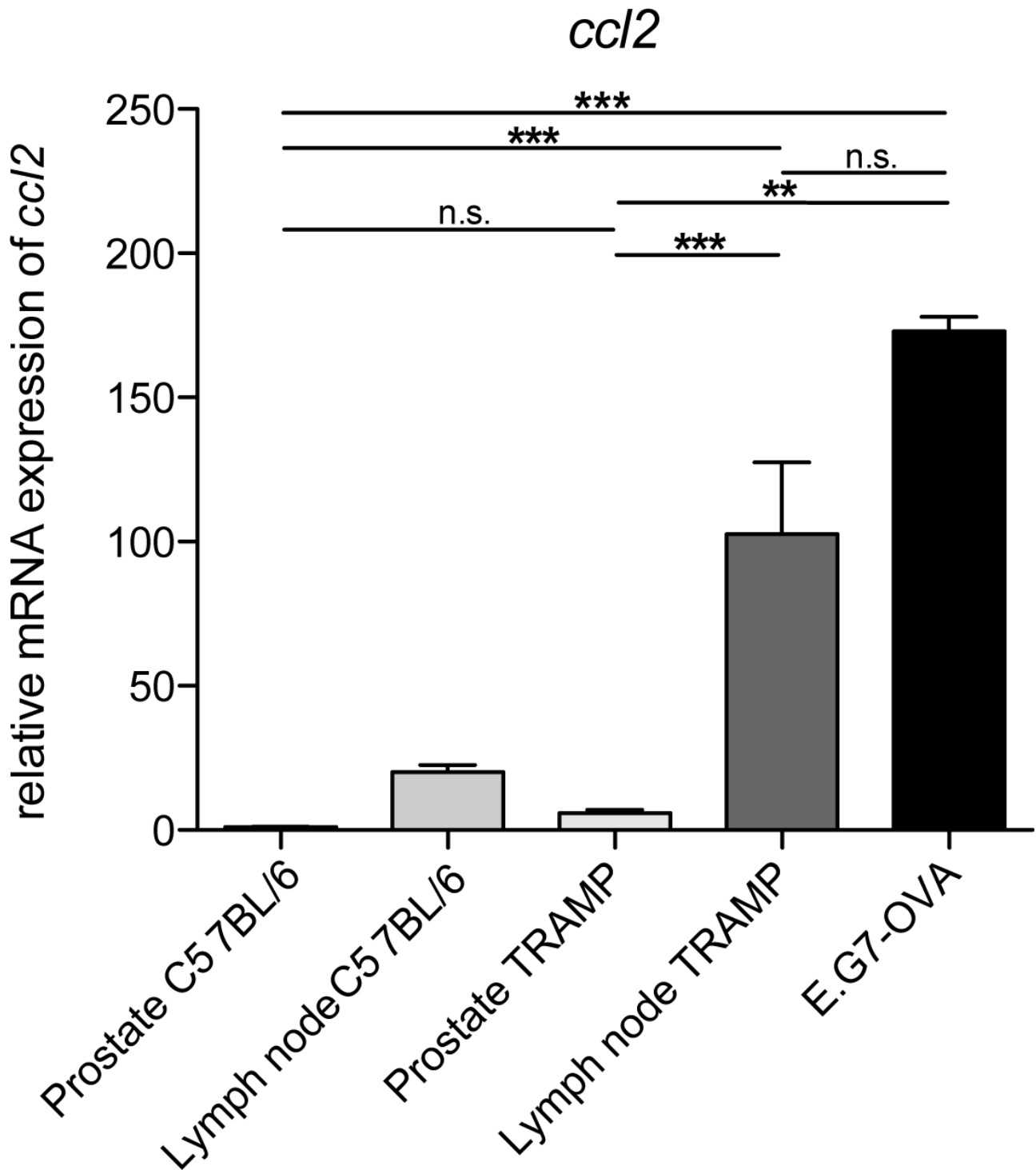
### Supplemental Figure 2

**A:** Chemokine expression in TRAMP primary tumors. *Ccl2*, *ccl5*, *cxcl12*, *cxcl9*, *cxcl10* and *cxcl11* mRNA relative expression in TRAMP or healthy prostate; Mann Whitney test: (\*) P<0.05; (\*\*) P<0.01; (ns) P>0.05. **B:** Transduction with CCR2 construct improves *in vitro* migration to CCL2. CCR2-transduced or control-transduced T cells were allowed to migrate toward CCL2 in a transwell assay. The migrated T cells were analyzed by FACS and the fold increase in migration is shown. Unpaired t test: (\*\*) P<0.01.



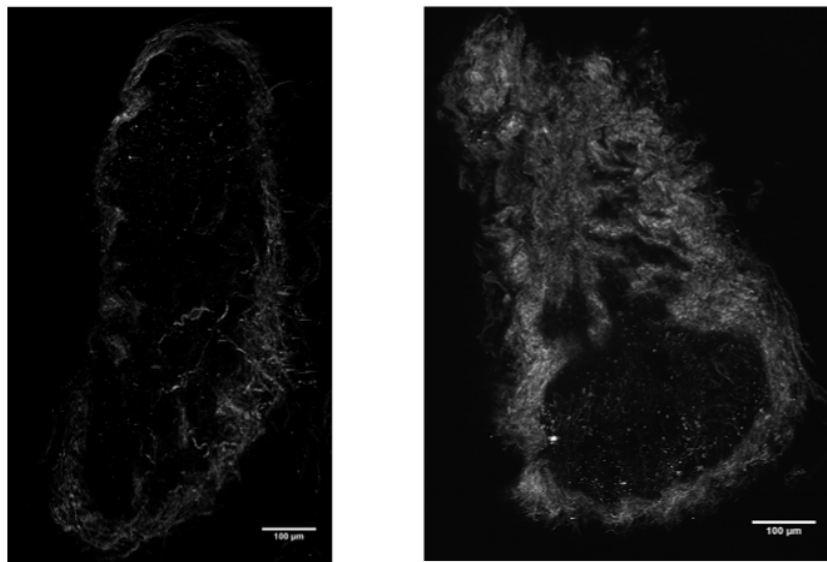
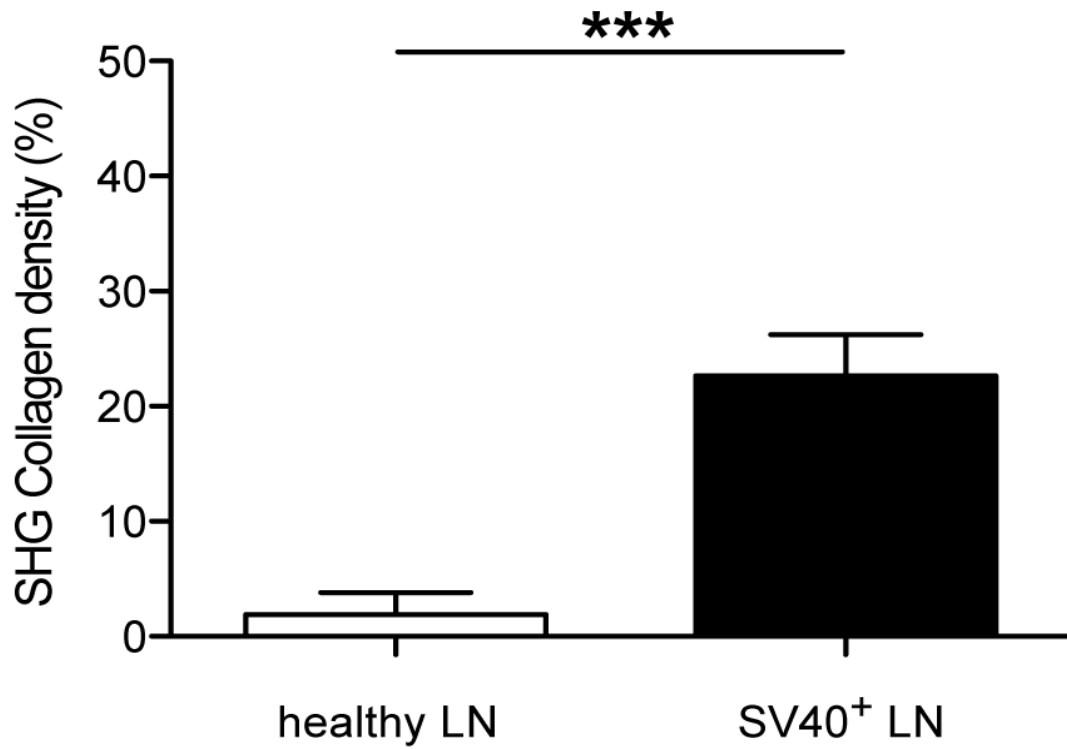
### Supplemental Figure 3

CCR2-transduced CD8<sup>+</sup> T cells in the metastatic lymph node are in contact with tumor cells. Representative image of immunohistochemical analysis of TRAMP SV40 TAg<sup>+</sup> metastatic lymph node sections from a recipient of CD8<sup>+</sup> T cells transduced with GFP-CCR2 and a TCR specific for SV40 TAg. Brown staining/red arrows: GFP<sup>+</sup> cells (GFP-CCR2<sup>+</sup> CD8<sup>+</sup> T cells). Blue staining/black arrows: SV40 TAg<sup>+</sup> (tumor) cells.



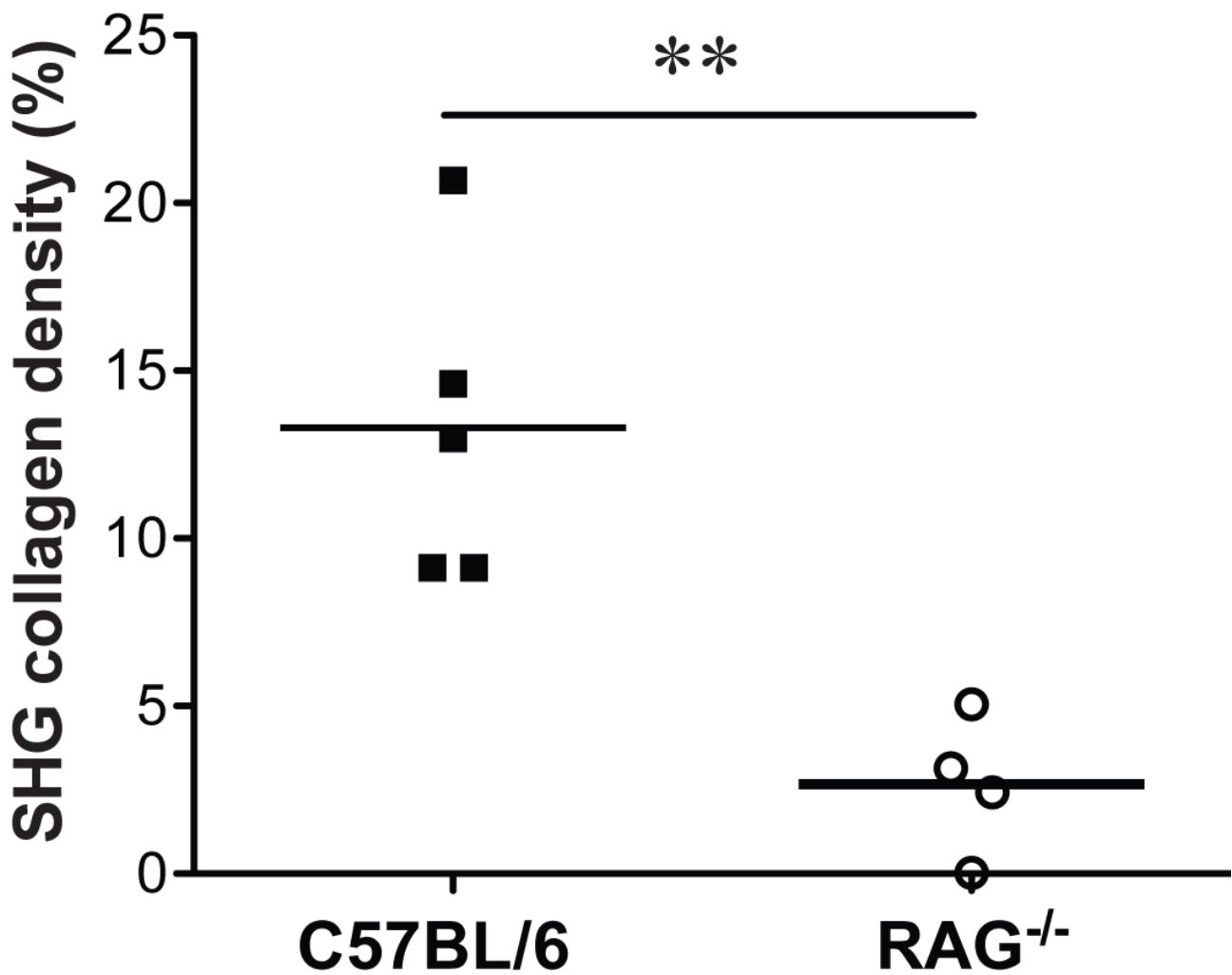
**Supplemental Figure 4**

*Ccl2* mRNA expression via qPCR on healthy C57BL/6 prostate tissue, healthy C57BL/6 lymph nodes, TRAMP prostate tumor and lymph nodes, E.G7-OVA lymphoma-derived implanted tumors. Data shown normalized to healthy prostate tissue; Non parametric 1-way ANOVA and Dunn's multiple comparison test: (\*\*\*)  $P < 0.001$ ; (\*\*)  $P < 0.01$ ; (ns)  $P > 0.05$ .



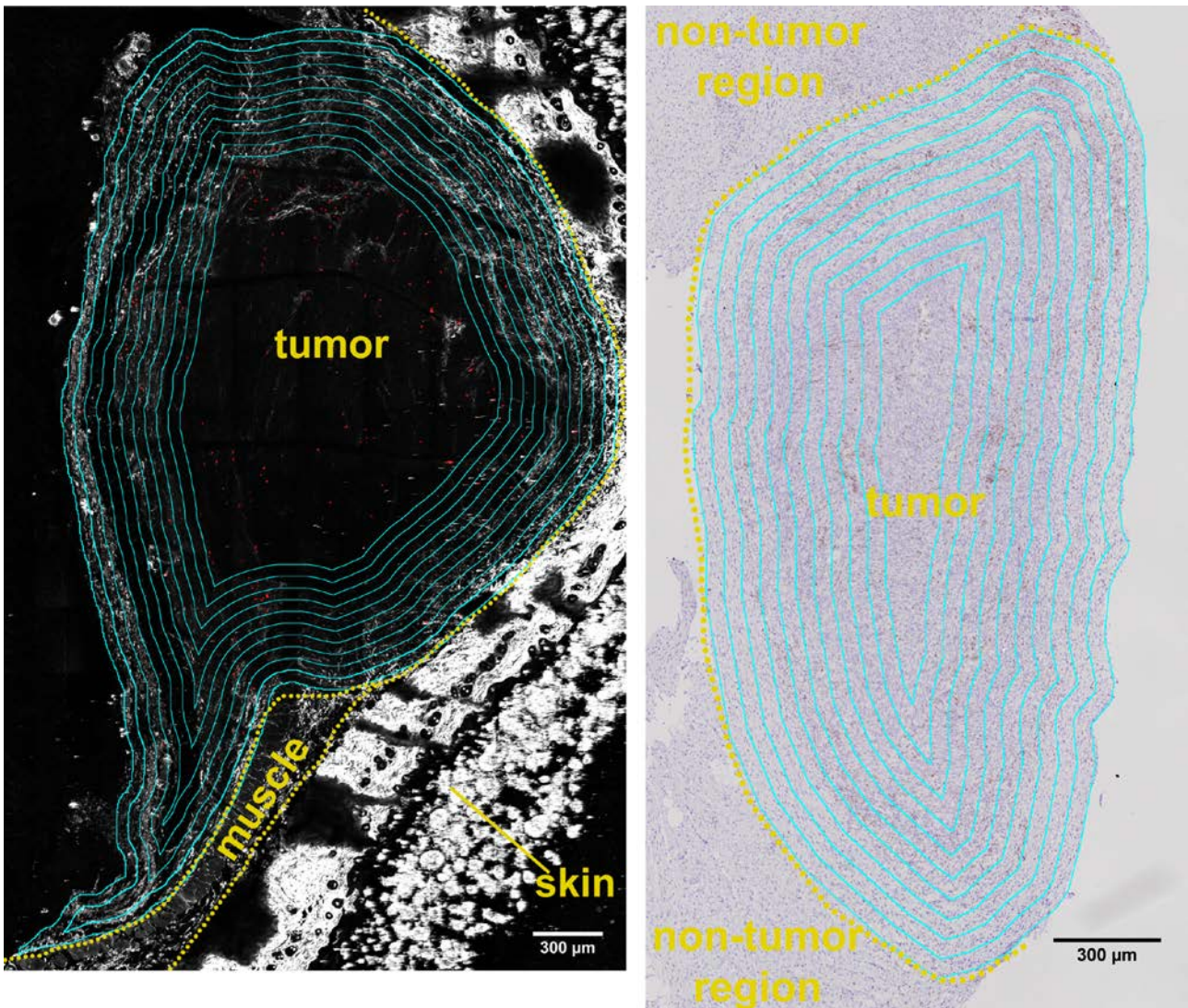
### Supplemental Figure 5

Metastatic lymph nodes show higher collagen density compared to healthy lymph nodes. Collagen density was evaluated by second harmonic generation (SHG) in 2-photon microscopy. Graph of collagen density in SV40 TAG<sup>+</sup> lymph nodes (n=9) or healthy lymph nodes (n=12); unpaired t test: (\*\*\*) P<0.001 (top). Representative images of SHG (shown in white) in SV40 TAG<sup>+</sup> and healthy lymph nodes (bottom).



**Supplemental Figure 6**

Host T cell presence favors fibrosis formation. Collagen density in the presence (C57BL/6 recipients) or absence (RAG<sup>-/-</sup> recipients) of host T cells was evaluated by second harmonic generation (SHG) in 2-photon microscopy; unpaired t test with Welch's correction: (\*\*) P<0.01; non-parametric t test (Mann-Whitney test; on the same data set) (\*) P<0.05.



### Supplemental Figure 7

Representative images of concentric regions of analysis of T cell distribution across the capsule. The image on the left is a 2-photon image of a tumor grown in a  $RAG^{-/-}$  recipient that received CMTMR-labeled T cells 3 days prior to harvesting. Red stain indicates T cell presence, white stain indicates collagen presence via SHG. The concentric regions start at the outer boundary of the peri-tumoral capsule and span 450  $\mu\text{m}$  into the tumor. The image on the right is an immunohistochemical analysis of a tumor grown in C57BL/6 recipients, which are T cell-sufficient. Brown staining indicates T cell presence. The concentric regions start at the outer boundary of the peri-tumoral capsule and span 450  $\mu\text{m}$  into the tumor.